AD-A144 035 PARAMETER ESTIMATION IN A CONSTRAINED STATE SPACE(U) 1/1
NAVAL UNDERWATER SYSTEMS CENTER NEWPORT RI
K F GONG ET AL. 28 JUN 84 NUSC-6286

UNCLASSIFIED F/G 12/1 NL

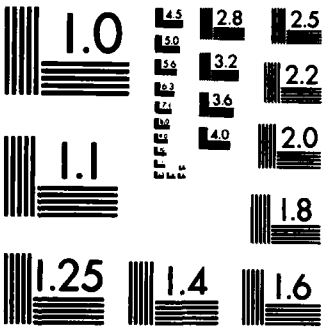

NUSC Reprint Report 6286
28 June 1984

Parameter Estimation in a Constrained State Space

Kai F. Gong
Antonio A. Magliaro
Steven C. Nardone

Combat Control Systems Department

Naval Underwater Systems Center
Newport, Rhode Island / New London, Connecticut

Reprint of an article published in the IEEE 1983 Conference Record of the Seventeenth Asilomar Conference on Circuits, Systems and Computers.

PARAMETER ESTIMATION IN A CONSTRAINED STATE SPACE

Kai F. Gong
Antonio A. Magliaro
Steven C. Nardone

U.S. Naval Underwater Systems Center
Newport, Rhode Island 02841

ABSTRACT

This paper examines the problems of state estimation for a moving acoustic source confined to a well-defined, simply-connected or multiply-connected region of state space. A multiple-parameter constrained estimator that provides enhanced performance and that permits determination of the most probable solution is presented. The estimator is a batch processor that yields both dynamic and residual classifiers, the behavior of which is shown to be dependent on source-observer geometry. The proposed realization is well-suited for solution selection through hypothesis testing. Experimental results showing estimator performance are presented and solution quality is discussed.

I. INTRODUCTION

In the underwater environment there are numerous situations in which a source is known to be confined to one of several, well-defined regions of the state space. Effective state estimation under these conditions requires that maximum use be made of all available information, and that some measure of solution quality be provided. Specifically, constraints on the state space environment are critical for problems characterized by large range-to-baseline ratios or high levels of measurement noise. Previous work has demonstrated that for the case where only bearing measurements involving high levels of "effective noise" are available, a phenomenon is experienced whereby significant deterioration in performance occurs with increasing range or noise level.[1,2] That study also examined estimation under a speed constraint and demonstrated significant improvement when such a priori information was included. Often, additional known parameters or knowledge of the physical constraints on some function of the source state components (such as a bound on range, speed, or depth) are available and should be exploited.

This paper addresses the problem of estimating the state and providing a measure of the quality of the solution for a source confined to a well-defined region of the state space. A multiple-parameter constrained estimator is presented for (1) enhancing the quality of estimates when a priori information constrains the state to a known (simply-connected) region, and (2) determining the most probable solution when the regions are distinct (multiply-connected).

When the source is known to be confined to a simply-connected region, it is possible to capitalize on such information via multiple-parameter constrained estimation. This is realized through augmentation of the information matrix by satisfying the Kuhn-Tucker conditions[3] or by treating the constraints as pseudo-measurements. Convergence is guaranteed by adaptively adjusting the weights of the constrained parameters.

When the source is known only to be confined in one of several possible well-defined finite regions, a parallel configuration with multiple constraints is presented. The configuration utilizes both dynamic and residual clues to classify the solution as to its most probable state space. The dynamic clue or classifier is defined in terms of a measure of deviation of the estimated velocity parameters from its expected range of values. Residuals are exploited by determination of expected variance and whiteness measures.

Under the above implementation, the ability to provide the most probable estimate of the state, or solution enhancement and a measure of solution quality, is dependent upon the amount of a priori information available. Experimental results demonstrating system performance for various cases outlined above are presented.

II. UNCONSTRAINED ESTIMATION

The problem under consideration involves the estimation of the position and velocity of a constant velocity acoustic source from noise-corrupted measurements. The source-observer scenario is illustrated in Figure 1. Let (r_{xT}, r_{yT}) and (r_{xO}, r_{yO}) be the positional components of the source and receiver, respectively. The discretized version of the dynamic process is given in Table 1. For the bearings-only case, the measurement is given by

$$z(k)=\beta(k)$$

$$=\tan^{-1}[[r_{xT}(k)-r_{xO}(k)]/[r_{yT}(k)-r_{yO}(k)]] \quad , \quad (1)$$

which represents a nonlinear model relating the noise-free measurements to the unknown source state. In (T-6), $\hat{x}_T$ is the estimated state at the selected reference time. Its value at any other time is determined via (T-1) and used in (1) to produce the appropriate bearing angle.

When the number of measurements, K, is greater than 4, (T-6) represents an overdetermined system of nonlinear equations. A weighted least-squares approach minimizes the norm of the residual vector

$$R_e = S^{-1}[Z_m - Z(\hat{x}_T)] \quad , \tag{2}$$

where $S=\text{Diag}[\sigma_{\beta k}]$, σ_β is the bearing measurement noise standard deviation, and $Z(\hat{x}_T)$ is the bearing sequence generated by the estimated state, $\hat{x}_T$, via (T-1), (T-4), and (1). The problem is complicated by the unusual observability properties of this system,[4] especially for long range scenarios.

The minimum of the norm-squared error,

$$J = [Z_m - Z(\hat{x}_T)]^T S^{-2} [Z_m - Z(\hat{x}_T)] \quad , \tag{3}$$

is found when the estimate $\hat{x}_T$ causes the gradient $G(\hat{x}_T)=\partial J/\partial \hat{x}_T$ to vanish; i.e.,

$$-1/2G(\hat{x}_T) = [\partial Z(\hat{x}_T)/\partial \hat{x}_T]^T S^{-1} [Z_m - Z(\hat{x}_T)] = [0]. \tag{4}$$

For Gaussian noise, the resulting $\hat{x}_T$ represents the maximum likelihood estimator (MLE). The premultiplying matrix is given by

$$[\partial Z(\hat{x}_T)/\partial \hat{x}_T] = \hat{R}^{-1} S^{-1} A(\hat{x}_T) \tag{5}$$

where

$$R^{-1} = \text{Diag}[r^{-1}(k)], \qquad k=1,2,\ldots,K \tag{6}$$

$$A(x_T) = \begin{bmatrix} \cos\beta_1 & -\sin\beta_1 & t_s\cos\beta_1 & -t_s\sin\beta_1 \\ \cos\beta_2 & -\sin\beta_2 & 2t_s\cos\beta_2 & -2t_s\sin\beta_2 \\ \vdots & \vdots & \vdots & \vdots \\ \cos\beta_K & -\sin\beta_K & Kt_s\cos\beta_K & -Kt_s\sin\beta_K \end{bmatrix} \Phi(t_0,t_R) \tag{7}$$

and where t_s is the data sampling period and $\Phi(t_0,t_R)$ is the transition matrix between the initial time, t_0 and reference time, t_R. The k^{th} element of the diagonal matrix of (6),

$$\hat{r}(k) = [[\hat{r}_{xT}(k) - r_{xO}(k)]^2 + [\hat{r}_{yT}(k) - r_{yO}(k)]^2]^{1/2}, \tag{8}$$

is the estimated range at the k^{th} instant, and

$$\hat{\beta}_k = \tan^{-1}[[\hat{r}_{xT}(k) - r_{xO}(k)]/[\hat{r}_{yT}(k) - r_{yO}(k)]] \tag{9}$$

in (7) is the corresponding bearing estimate. Hence, one seeks to solve the nolinear set of equations

$$A^T(\hat{x}_T)\hat{R}^{-1}S^{-2}[Z_m - Z(\hat{x}_T)] = [0] \tag{10}$$

for $\hat{x}_T$. Employing the Gauss-Newton iterative method[5] to solve (10) yields

$$\hat{x}_{j+1} = \hat{x}_j + \delta_j [\hat{A}_j^T \hat{R}_j^{-2} S^{-2} \hat{A}_j]^{-1} \hat{A}_j^T \hat{R}_j^{-1} S^{-2} Z_e \quad , \tag{11}$$

where $\hat{A}_j$ and Z_e are evaluated at $\hat{x}_j$, and the step size, δ_j, is selected at each iteration to ensure convergence.

Equation (11) represents the solution for the unconstrained maximum likelihood estimator. Performance of the estimator has been assessed by examination of the ideal information matrix, or Cramer-Rao bound, for large range-to-baseline geometries.[1] In this situation, the assumptions of constant range and symmetric geometry are valid. Under these conditions, the eigenvalues of the ideal information matrix are given in the second column of Table 2.[1] Note that significant deterioration in performance occurs with increasing range or noise level.

III. ESTIMATION IN CONSTRAINED STATE SPACE

Since errors in the estimates of range and range rate are inversely proportional to λ_{R_M} and $\lambda_{\dot{R}_M}$, respectively, it is seen from Table 2 that variations in these estimates significantly increase for large values of "effective noise," $r\sigma_\beta/B$, where B denotes synthetic baseline. When unreasonable estimates result, a priori information or heuristic data can be utilized to advantage. Often, known parameters or knowledge of the physical constraints on some functions of the state components are available and should be exploited. Under these conditions, the problem then becomes one of minimizing the cost function

$$J = [Z_m - Z(\hat{x}_T)]^T S^{-2} [Z_m - Z(\hat{x}_T)] \quad , \tag{12}$$

subject to the constraint

$$f(\hat{x}_T) \le b \quad . \tag{13}$$

Here, $f(\hat{x}_T)$ and b denote the vectors $[(f_1, f_2, \ldots, f_N)]^T$ and $[(b_1, b_2, \ldots, b_N)]^T$, respectively, and N is the number of constraints. Denoting $f_i = \pm HM_i \hat{x}_T M^2$, the necessary and sufficient conditions for J to be minimum is given by the Kuhn-Tucker conditions.[2,3] That is,

$$\hat{x}_{j+1} = \hat{x}_j + \delta_j \{\hat{A}_j^T \hat{R}_j^{-2} S^{-2} \hat{A}_j \pm \sum_{i=1}^{N} \rho_i M_i^T M_i\}^{-1} \cdot \{\hat{A}_j^T \hat{R}_j^{-1} S^{-2} Z_e \pm \sum_{i=1}^{N} \rho_i^T M_i^T M_i \hat{x}_j\} \tag{14a}$$

$$\rho_i [b_i - f_i(\hat{x}_{j+1})] = 0 \qquad i=1,2,\ldots,N \tag{14b}$$

$$\rho_i \ge 0 \qquad i=1,2,\ldots,N \tag{14c}$$

$$f_i(\hat{x}_{j+1}) \le b_i \qquad i=1,2,\ldots,N \quad , \tag{14d}$$

where $\rho_i, i=1,2,\ldots,N$ is a scalar to be determined. For the single parameter constraint case, ρ can be shown to be conveniently computed iteratively[2] via

$$\rho_{j+1} = \rho_j + \Delta\rho \tag{15}$$

where

$$\Delta\rho = 0.5\{[f(\hat{x}_T) - b]/[W^T P_W W]\} \cdot \{f(\hat{x}_T)/[f(\hat{x}_T) + d|f(x_T) - b|]\} \quad , \tag{16}$$

and where W is the state vector associated with $f(\hat{x}_T)$, P_W is its covariance, and d is selected to ensure system stability. Multiple parameter

constraints can be realized by either sequential or simultaneous processing via (14). For the case of single parameter constraint, experiments have shown satisfactory convergence and stability for both speed and depth constraint[2,6]. For the case of speed constraint, an improvement factor of 2 in localization error has been demonstrated.

An alternative implementation of estimation in a constrained state space is to consider the constraints as "pseudo-measurements." If the measurement vector is given by

$$Z_p=[Z_m,b]^T+n \quad , \tag{17}$$

the cost function then becomes $J_p=J+J_b$ where

$$J_b=[b-f(\hat{x}_T)]^T\rho^{-2}[b-f(\hat{x}_T)], \tag{18}$$

subject to the constraints of (13). The solution is obtained by finding an $\hat{x}_T$ such that J_p is minimized. Setting the gradient $\partial J_p/\partial \hat{x}_T$ equal to zero and employing the Gauss-Newton iterative method yields

$$\hat{x}_{j+1}=\hat{x}_j+\delta_j\{(\hat{A}_j^T\hat{R}_j^{-2}S^{-2}\hat{A}_j]^{-1}\hat{A}_j^T\hat{R}^{-1}S^{-2}Z_e + \sum_{i=1}^{N}[\hat{A}_{bi}^T\rho_i^{-2}\hat{A}_{bi}]^{-1}\hat{A}_{bi}^T\rho_i^{-2}[b_i-f(\hat{x}_j)]\} \quad , \tag{19}$$

or

$$\hat{x}_{j+1}=\hat{x}_j+\delta_j(\hat{\Omega}_j^TQ_j^{-2}\hat{\Omega}_j)^{-1}\hat{\Omega}_j^TQ_j^{-1}Z_{pe}, \tag{20}$$

where Ω is the modified infcrmation matrix given by

$$\hat{\Omega}=\hat{A}^T\hat{R}^{-2}S^{-2}\hat{A} + \sum \hat{A}_{bi}^T\rho_i^{-2}\hat{A}_{bi} \tag{21}$$

and

$$A_b=\partial f(\hat{x}_T)/\partial \hat{x}_T \quad , \tag{22}$$

$$Q=\mathrm{Diag}[\sigma_{\beta k},\rho_i], \tag{23}$$

$$Z_{pe}=\{Z_e^T\,[b-f(\hat{x}_T)]^T\}^T \quad , \tag{24}$$

and where $\rho_i>0$ and is either known or can be determined adaptively via

$$\rho_{ij}^2=\rho_{0i}^2/j \qquad j=1,2,\ldots \tag{25}$$

until the constraints are satisfied. Experiments conducted utilizing (20) for the speed constraint have yielded equivalent results to those obtained via (14). Although the use of (14) for range constraint under adverse conditions has experienced some cases of slow rate of convergence, (20) has provided stable and rapid solutions. Note, however, that (20) represents the solution of an unbiased estimator; as such the modified information matrix (or its inverse) must be interpreted appropriately consistent with the a priori data description. When insufficient description on the data-weighting assignment is available, the modified information matrix can be more appropriately generated by applying (14), or in the case of slow convergence by utilizing the speed solution of (20) as the constrained parameter and then applying (14). Further comparison of (14) and (20) in regard to their robustness, and analysis of the mechanisms that impact the estimate will be addressed in future studies.

IV. CONSTRAINED ESTIMATION IN SIMPLY-CONNECTED REGIONS

When a priori information constrains the source to a known region (simply-connected), performance can be significantly improved. This can be demonstrated by examining the augmented information matrix of (21) when range information, with standard deviation, σ_R, is available at K. Under this condition,

$$\Omega(t_R)=\hat{A}^T\hat{R}^{-2}S^{-2}\hat{A} + \hat{A}_R^T\sigma_R^{-2}\hat{A}_R \tag{26}$$

where

$$\hat{A}_R=\begin{bmatrix} 0 & 0 & 0 & 0 \\ \vdots & \vdots & \vdots & \vdots \\ 0 & 0 & 0 & 0 \\ \cos\hat{\beta}_K & \cos\hat{\beta}_K & Kt_s\sin\hat{\beta}_K & Kt_s\cos\hat{\beta}_K \end{bmatrix}\Phi(t_0,t_R) \tag{27}$$

Assuming uniform signal-to-noise ratio, the augmented information matrix at K/2 becomes

$$\Omega=\sum_{-K/2}^{K/2}\begin{bmatrix} \Omega_k & (k-K/2)\Omega_k \\ (k-K/2)\Omega_k & (k-K/2)^2\Omega_k \end{bmatrix}+\begin{bmatrix} \Omega_R & (K/2)\Omega_R \\ (K/2)\Omega_R & (K/2)^2\Omega_R \end{bmatrix}, \tag{28}$$

where

$$\Omega_k=\frac{1}{r_k^2\sigma_\beta^2}\begin{bmatrix} \cos^2\hat{\beta}_k & -\sin\hat{\beta}_k\cos\hat{\beta}_k \\ -\sin\hat{\beta}_k\cos\hat{\beta}_k & \sin^2\hat{\beta}_k \end{bmatrix} \tag{29}$$

and

$$\Omega_R=\frac{1}{\sigma_R^2}\begin{bmatrix} \sin^2\hat{\beta}_K & \sin\hat{\beta}_K\cos\hat{\beta}_K \\ \sin\hat{\beta}_K\cos\hat{\beta}_K & \cos^2\hat{\beta}_K \end{bmatrix} . \tag{30}$$

Using the assumption of symmetric geometry, $\Omega(K/2)$ is diagonalized;[1] that is,

$$E[\Omega_k] = \begin{bmatrix} \cos^2\hat{\beta}_k & 0 \\ 0 & \sin^2\hat{\beta}_k \end{bmatrix} / r_k^2\sigma_\beta^2 \tag{31}$$

and

$$E[\Omega_R] = \begin{bmatrix} \sin^2\hat{\beta}_K & 0 \\ 0 & \cos^2\hat{\beta}_K \end{bmatrix} / \sigma_R^2 . \tag{32}$$

For long range scenarios, the range is assumed to be essentially constant; i.e., R=rI. Under these conditions, the expected eigenvalues of $\Omega(K/2)$ are given in Table 2. The variance is given by the reciprocal of the eigenvalue, or

$$\sigma_\mu^2 = \frac{\sigma_\mu^2(\beta)\sigma_\mu^2(R)}{\sigma_\mu^2(\beta)+\sigma_\mu^2(R)} \quad , \qquad \mu=R_\perp,R_\parallel,\dot{R}_\perp,\dot{R}_\parallel \tag{33}$$

where $\sigma_\mu^2(p)$ is the variance of μ due to the parameter p alone. Clearly, if range information is given, the expected improvement factor in the reduction of variance over bearings-only processing is $[\sigma_\mu^2(\beta)+\sigma_\mu^2(R)]/\sigma_\mu^2(R)$. Equation (33) can be generalized when multiple parameters are known a priori and $\Omega(K/2)$ is diagonalizable to yield

$$\sigma_\mu^2 = \frac{\sigma_\mu^2(\beta)}{1+\sigma_\mu^2(\beta)\sum_i \sigma_\mu^{-2}(p_i)} \quad , \tag{34}$$

resulting in an improvement factor of $[1+\sigma_\mu^2(\beta)\Sigma_i\sigma_\mu^{-2}(p_i)]$. Further analysis on the impact of additional information is contained in reference 7.

V. PROPERTIES OF ESTIMATION IN CONSTRAINED STATE SPACE

Based on the analysis in the previous section, the availability of a priori information, heuristic or otherwise, can clearly provide improvement in system performance. However, in many situations, such as the one in which the source is known only to be confined to one of several distinct regions (multiply-connected), only limited heuristic information is available. Under these conditions, improvement in state estimation is still possible by providing the most probable solution.

Consider the relation for cross-range-rate component

$$R\dot{\beta}=S_T\sin(C_T-\beta)-S_O\sin(C_O-\beta) \tag{35}$$

where $\dot{\beta}$ is the bearing rate, S_T and S_O are source and observer speed, respectively, and C_T and C_O represent source and observer course, respectively. Let $(\hat{S}_T,\hat{C}_T,\hat{\dot{\beta}},\hat{\beta})$ be the estimate obtained by constraining the range at $\hat{R}_C$. The variation of speed as a function of range can be analyzed by perturbing (35) to yield

$$\Delta S/\Delta R=(\hat{\dot{\beta}}+\hat{R}_C\Delta\hat{\dot{\beta}}/\Delta\hat{R}_C)/\sin\hat{\theta}-[\Delta\hat{\theta}/\Delta\hat{R}_C][(\hat{S}_T+\Delta S)/\tan\hat{\theta}] \tag{36}$$

where $\hat{\theta}=\hat{C}_T-\hat{\beta}$ and the assumption is made that $\Delta\beta/\Delta\hat{R}_C=0$. Generally, $\hat{\theta}(R)$ is point symmetrical about $(\underline{R},\underline{\theta})$ and can be approximated as piecewise linear (Figure 2). The quantity $\Delta\theta/\Delta\hat{R}_C$ can be treated as a constant, k_1, within the interval (R_1,R_2). Therefore, the slope of the speed-range function can be rewritten as

$$\Delta S/\Delta R_C=[(\hat{\dot{\beta}}+\hat{R}_C\Delta\hat{\dot{\beta}}/\Delta\hat{R}_C)-k_1\hat{S}_T\cos\hat{\theta}]/(\sin\hat{\theta}+\Delta\hat{\theta}\cos\hat{\theta}). \tag{37}$$

Clearly, $\hat{\theta}$ is geometry and noise dependent and is inversely related to the slope. As $\hat{\theta}$ increases, the change in the speed estimate is less senstive to range. The minimum speed can be computed about $(\underline{R},\underline{\theta})$ by setting (37) to zero to yield

$$\hat{S}_{min}=(\hat{\dot{\beta}}+\hat{R}_C\Delta\hat{\dot{\beta}}/\Delta\hat{R}_C)/k_2\cos\hat{\theta} \tag{38}$$

where k_2 is generally large for small θ. Consequently, geometries with small θ generally have smaller S_{min}.

Thus, (37) and (38) provide the expected dynamic behavior of source estimates. This is illustrated in Figure 3. The solution, dependent on the noise conditions, may fall anywhere along the speed-range curve. However, if the maxium speed, S_{max}, is known a priori, the most probable solution must then be bounded by S_{max} and S_{min} and, therefore, is confined to R as shown in Figure 4. If, in addition, the source is known to be in either R_1 or R_2, knowledge of S_{max} then can eliminate R_2 as a possible solution.

Further insight can be gained by analyzing the effects of constraining the estimates away from the speed-range function. This corresponds to performing estimation with range and speed constraints. Thus, given the estimate $(\hat{S}_T,\hat{R})$, and if the parameters are constrained to $(\hat{S}_T,\hat{R}+\Delta R)$, (35) then becomes

$$(\hat{R}+\Delta R)(\hat{\dot{\beta}}+\Delta\hat{\dot{\beta}})=\hat{S}_T\sin(\hat{\theta}+\Delta\theta)-S_O\sin(\hat{\gamma}+\Delta\gamma) \quad , \tag{39}$$

where $\hat{\gamma}=C_O-\hat{\beta}$. Assuming small $\Delta\theta$ and $\Delta\gamma$, the resulting bearing rate error, $\Delta\hat{\dot{\beta}}$, can be approximated as

$$\Delta\hat{\dot{\beta}}=[(\hat{S}_T/\hat{R})\Delta C(1-\Delta C/2)\cos\hat{\theta}-(\Delta\beta\hat{\dot{R}}/\hat{R}+\hat{\dot{\beta}}\Delta R/\hat{R})]/(1+\Delta R/\hat{R}), \tag{40}$$

where ΔC is the change in $\hat{C}_T$ corresponding to ΔR.

Equation (40) represents the slope of the residual, and can easily be computed for each leg of constant observer velocity. Furthermore, it provides a measure of inconsistency and sensitivity in the state estimates. Such a measure can be used in conjunction with the expected residual variance, as given by (3), to supply a more extensive description of the residuals. To a certain extent, (3) and (40) provide a "whiteness" measure. This measure can alternatively be obtained by performing a spectral analysis on the residuals. Similar analysis can be performed for different constraint combinations or with additional constraints.

Thus, when a priori information constrains the source to one of several possible solution regions, or when limited heuristic data are available, the estimation configuration of Figure 5 can be employed along with (37), (38), (3), and (40) to provide the most probable solution.

VI. GENERAL OBSERVATIONS, SOLUTION QUALITY, AND SELECTION

The analysis presented up to this point deals with the problem of estimating the state parameters by capitalizing on any available a priori information. Depending on geometry and amount of information (heuristic or otherwise), constrained estimation can provide enhancement in the target state estimates either by reducing the state error variances or by providing the most probable solution(s). Some general observations are summarized as follows:

1. The speed-range relation of Figure 2 is derived by minimizing the cost function, J, and is geometry dependent. The slope and minimum speed are predictable and can be analyzed via (37) and (38). For geometries that exhibit stronger across-the-line-of-sight component, the magnitude of the

speed-range slope is smaller and the minimum speed is larger; furthermore, the residuals are more sensitive to deviations from the solution curve.

2. The availability of valid a priori information (e.g., range, speed, course) will provide enhanced estimates with reduced state error variance, consistent with respect to both dynamic and residual behaviors.

3. The availability of valid speed or range information will enable the selection or determination of the most probable solution based on dynamic and residual consistency tests.

4. The dynamic behavior curve can potentially be applied to determine the approximate dynamic behavior of the process.

5. In the absence of other information, the physical constraint of maximum allowable speed and the predicted minimum speed can be employed to bound the solution heuristically. In addition, both dynamic and residual clues can be employed to determine a solution region.

Based on the preceding observations, estimation via the constrained approach provides improvements in system performance. Given a state estimate from an algorithm, the dynamic and residual clues can provide a check on its validity. In addition, the constrained estimation approach provides the mechanisms that maximize the use of any available a priori information. Furthermore, it can be employed for solution selection.

Theoretically, the covariance matrix provides a statistical measure of solution quality assessment, although its validity is algorithm dependent. The predictable dynamic and residual behaviors and solution bounds provided by constrained estimation clearly can be used as heuristic solution quality measures; and, when used in conjunction with the covariance matrix, can provide a viable means for solution quality assessment and solution selection.

VII. SIMULATION RESULTS AND DISCUSSION

Experiments were conducted using the geometries of Figure 1. A total of six geometries were considered. A normalized observer speed (S_O/S_{max}) of 0.47 was employed. Source dynamics are given in Table 3. Zero mean Gaussian noise with 2° standard deviation was added to the true bearing. A total of 400 equispaced measurements were collected on each leg. All subsequent discussion is referenced to the final time.

Figures 6 and 7 show the behavior of speed and course estimates as a function of the constrained range for different $\theta=C_T-\beta$. The unconstrained MLE estimates are also included for completeness. As shown, the dynamic behavior is geometry dependent. At the center portion of the course-range plot, the magnitude of the slope increases as the angle θ decreases. Consequently, the geometry with the smallest θ exhibits the smallest minimum speed, as shown in Figure 6 (see (38)); also, the speed-range slope is much sharper with smaller θ geometry since it varies inversely with $\sin\theta$ and $\cos\theta$ (see (37)). For the approximately symmetric source-observer geometries considered, the estimated course function is approximately point symmetric about the point at $R_C[S_{min}(\hat{\theta})]$ where $\hat{C}_T=90°$. In the case where θ is near zero, the 180° difference in the estimated course corresponding to ranges on either side of $R_C[S_{min}(\hat{\theta})]$ is reflected by a switch of sign for the slope of the speed-range curve. As θ increases, the last term of (37) dominates; thus, the symmetric change of the estimated course about 90° in Figure 7 leads to slopes for the speed-range plot which are equal in magnitude but opposite in sign. This dynamic behavior is illustrated in Figure 8 where a total of 30 noise sequences have been applied.

Sensitivity of the state estimates is examined by perturbing the range or speed estimate and by monitoring the resulting residuals. The results are shown in Figures 9 and 10. The shaded area of Figure 9 represents solutions which yield approximately the same value of residual variance, $\hat{\sigma}_\beta^2$. In essence, this area can be viewed as a region of minimal $\hat{\sigma}_\beta^2$; therefore, estimates located outside the shaded region may yield residuals which are statistically inconsistent and which should be rejected as possible solutions. This situation is illustrated in Figure 10 when constraints were imposed by utilizing an incompatible range-speed combination. In fact, the residuals have the functional form $e_t=e_{t0}+\Delta\dot{\beta}_t T_t+\beta_{et}$, where T_t denotes the length of the t^{th} leg, e_{t0} is the referenced initial residual, and β_{et} is the random component. For the noise free case, the slope $\Delta\dot{\beta}_t$ agrees well with that given by (40). Thus, if incompatible a priori information is employed, clues from the residuals, such as $\hat{\sigma}_\beta^2$ and $\Delta\dot{\beta}_t$, can potentially be utilized to reject any invalid estimate. In this context, both dynamic and residual clues can be applied advantageously for solution quality assessment.

The improvement obtainable when good information is utilized for constrained estimation is illustrated in Figure 11. In this figure, it can be seen that when the range, $R_C\pm\sigma_R$, or speed is given as heuristic data, the constrained estimator provides significant improvement in solution accuracy and solution uncertainty reduction. Solution consistency is confirmed by both the dynamic behavior and the residuals.

Estimation for the situation when the source is known to be in one of three regions is demonstrated in Figures 12 and 13. Information is also available (with probability 1) in regard to the source's maximum speed. The configuration of Figure 5 is employed by constraining range to each respective region with and without the additional speed constraint. For the case of constraining only range, hypothesis testing of maximum speed is employed, and the results show that the region, denoted by R_1, is the true solution. For the case of constraining both range and speed, the residual clues of Figures 13a-c again provide the necessary information to select R_1 as the most probable solution.

VIII. SUMMARY AND CONCLUSION

The problem of parameter estimation in a constrained state space that capitalizes on the utilization of a priori information (or heuristic data) was presented. A nonlinear estimator with multiple constraints was considered and its properties analyzed. The estimator is a batch processor that yields both dynamic and residual characteristics which permit solution enhancement, solution selection, and quality assessment. Sensitivity of these characteristics is shown to depend on source-observer geometry. Dynamic clues are common for low bearing rate trajectories, while residual clues are most evident in scenarios having a noticeable across-the-line-of-sight velocity component. While the ability to determine the state parameters via acoustic measurement processing becomes increasingly difficult with deteriorating conditions, effective utilization of a priori information is shown to provide significant enchancement. When the source is known to be confined in a well-defined region, enhancement is realized by reducing the solution error variance. When the a priori information or heuristic data constrain the source in one of several regions, the estimator is capable of providing the most probable solution. In addition, both dynamic and residual clues are predictable. These, when used in conjunction with the estimated state covariance matrix, can provide a viable measure of solution quality.

REFERENCES

1. S.C. Nardone, A.G. Lindgren, and K.F. Gong, "A Performance Analysis of Some Passive Bearings-Only Target Tracking Algorithms," 15th Asilomar Conference on Circuits, Systems and Computers, November 1981.

2. K.F. Gong, S.C. Nardone, and A.G. Lindgren, "Passive Localization and Motion Analysis With a State Parameter Constraint," 15th Asilomar Conference on Circuits, Systems and Computers, November 1981.

3. Maxwell Noton, Modern Control Engineering, Pergamon Press, Inc., New York, 1972.

4. S.C. Nardone and V.J. Aidala, "Observability Criteria for Bearings-Only Target Motion Analysis," IEEE Transactions on Aerospace and Electronic Systems, Vol AES-17, No. 2, March 1981.

5. G. Dahlquist and A. Bjork [translated by N. Anderson], Numerical Methods, Prentice Hall, 1974.

6. K.F. Gong, S.E. Hammel, S.C. Nardone, and A.G. Lindgren, "Utilization of Environmentally Perturbed Acoustic Measurements for Three-Dimensional Target Parameter Estimation," 16th Asilomar Conference on Circuits, Systems and Computers, November 1982.

7. S.C. Nardone, A.G. Lindgren, and K.F. Gong, "Measurements, Information, and Target Motion Analysis," 17th Asilomar Conference on Circuits, Systems, and Computers, November 1983.

Table 1. System Dynamics and Measurements

Source States

$$x_T(k+1) = \Phi(k+1,k)x_T(k) \quad \text{(T-1)}$$

$$x_T(k) = [r_{xT}(k)\ r_{yT}(k)\ V_{xT}(k)\ V_{yT}(k)]^T \quad \text{(T-2)}$$

$$\Phi = \left[\begin{array}{c|c} I & t_s I \\ \hline 0 & I \end{array}\right] \quad \text{(T-3)}$$

Observer States

$$x_O(k+1) = \Phi(k+1,k)x_O(k) + \Delta(k) \quad \text{(T-4)}$$

(where $\Delta(k)$ accounts for effects of maneuver)

$$x_O(k) = [r_{xO}(k)\ r_{yO}(k)\ V_{xO}(k)\ V_{yO}(k)]^T \quad \text{(T-5)}$$

Measurement Vector

$$Z_m = Z(x_T)+\eta \quad \text{(T-6)}$$

$$Z = [z_1, z_2, \ldots, z_K]^T \quad \text{(T-7)}$$

$$\eta = [\eta_1, \eta_2, \ldots, \eta_K]^T \quad \text{(T-8)}$$

$$E[\eta] = [0] \quad \text{(T-9)}$$

$$E[\eta\eta^T] = \text{Diag}[\sigma_{zk}^2],\ k=1,2,\ldots,K \quad \text{(T-10)}$$

Table 2. Eigenvalues of $\Omega(K/2)$ via Processing Bearing (with Range Constraint)

$$\lambda_\mu = \lambda_\mu(\beta)+\lambda_\mu(R),\ \mu = \dot{R}_\perp, R_\perp, R_\parallel, \dot{R}_\parallel$$

μ	$\lambda_\mu(\beta)$	$\lambda_\mu(R)$
$\dot{R}_\perp$	$(K^3/12)(1/r^2\sigma_\beta^2)$	$(K/2)^2(\theta^2/12)(1/\sigma_R^2)$
$\dot{R}_\parallel$	$(K^3\theta^2/144)(1/r^2\sigma_\beta^2)$	$(K/2)^2(1/\sigma_R^2)$
$R_\perp$	$K/r^2\sigma_\beta^2$	$(\sigma^2/12)(1/\sigma_R^2)$
$R_\parallel$	$(K\theta^2/12)(1/r^2\sigma_\beta^2)$	$1/\sigma_R^2$

Where $\lambda_\mu(\cdot)$ is the eigenvalue of the μ-component due to $(\cdot)$; $R_\perp$ and $\dot{R}_\perp$ are range and range-rate components perpendicular to the line of sight; and $R_\parallel$ and $\dot{R}_\parallel$ are range and range-rate components along the line of sight.

Table 3. Source Trajectory Parameters

Geom	Course (Deg)	$\theta_i = C_{Ti} - \beta_i$ (Deg)	Normalized Speed/Range
1	0	1.25	
2	20	17.8	$S/S_{max} = 0.67$
3	45	38.9	$R_1/B = 9.5$
4	80	70.1	
5	90	83.0	$S/S_{max} = 0.67$ $R_1/B = 9.5$
6	90	66.4	$S/S_{max} = 0.67$ $R_2/B = 4.0$

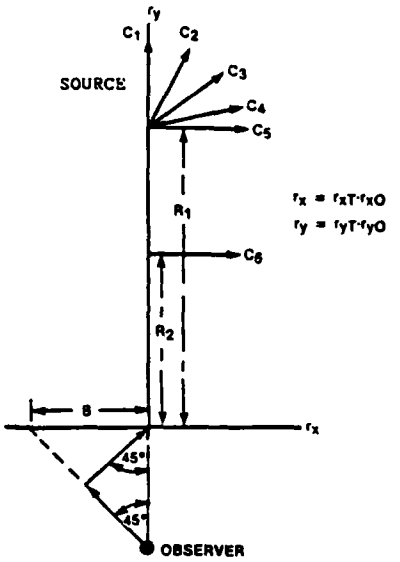

Figure 1. Source-Observer Geometries

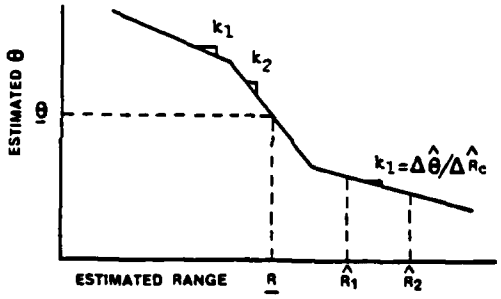

Figure 2. Experimentally Observed Behavior for $\theta = C_T - \beta$

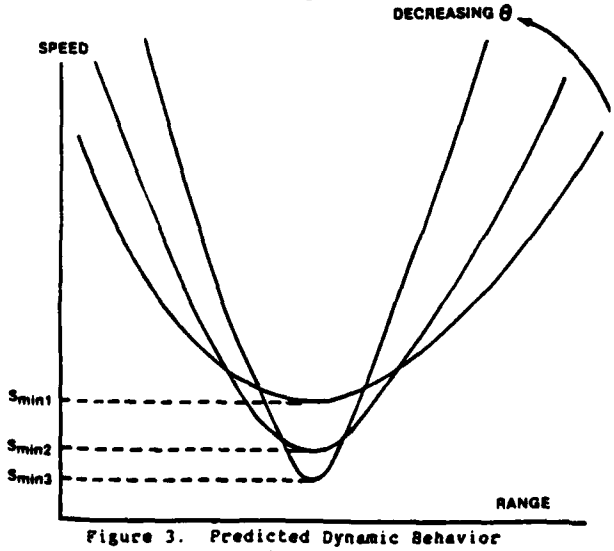

Figure 3. Predicted Dynamic Behavior in Constrained Estimation

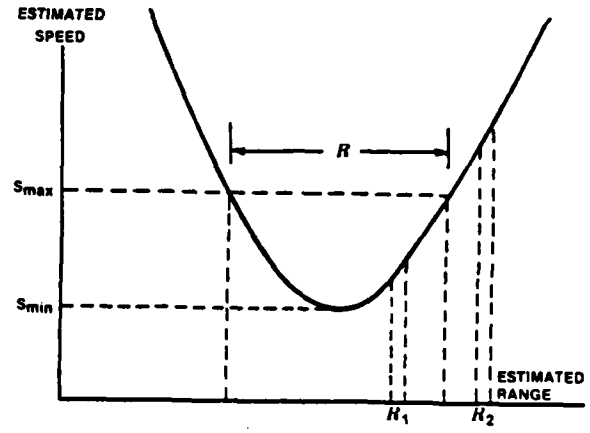

Figure 4. Potential Application of Constrained Estimation: Solution Selection

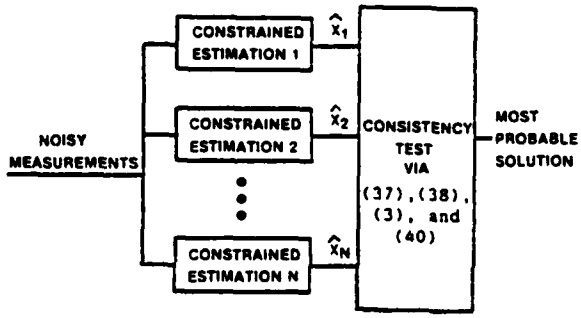

Figure 5. Estimation Configuration with Limited A Priori Information (Multiply-Connected Region)

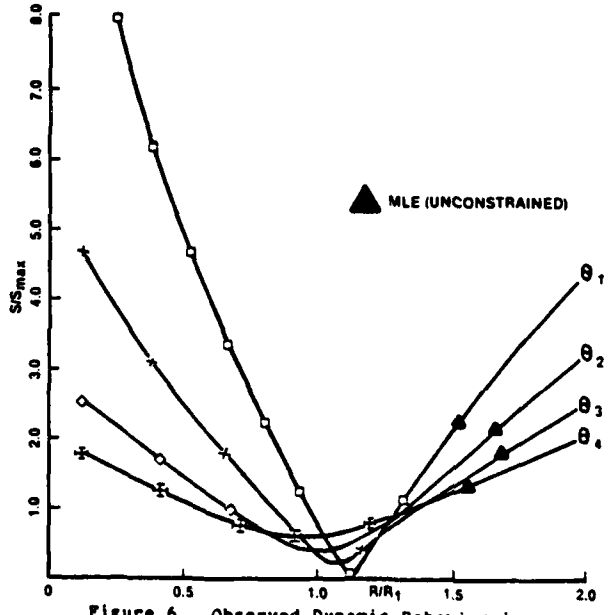

Figure 6. Observed Dynamic Behavior in Constrained Estimation: Normalized Speed vs Normalized Range Constraint

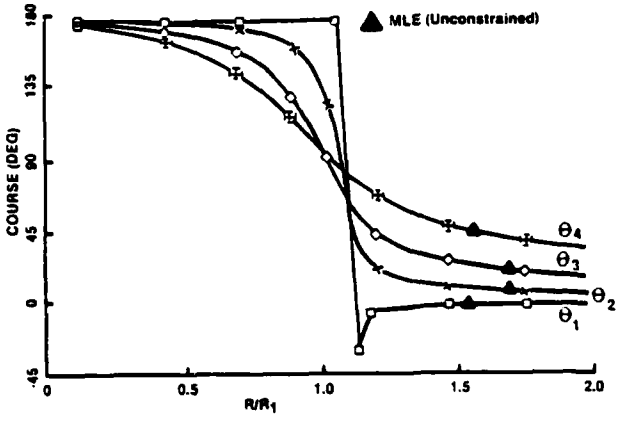

Figure 7. Observed Dynamic Behavior in Constrained Estimation: Course vs Normalized Range Constraint

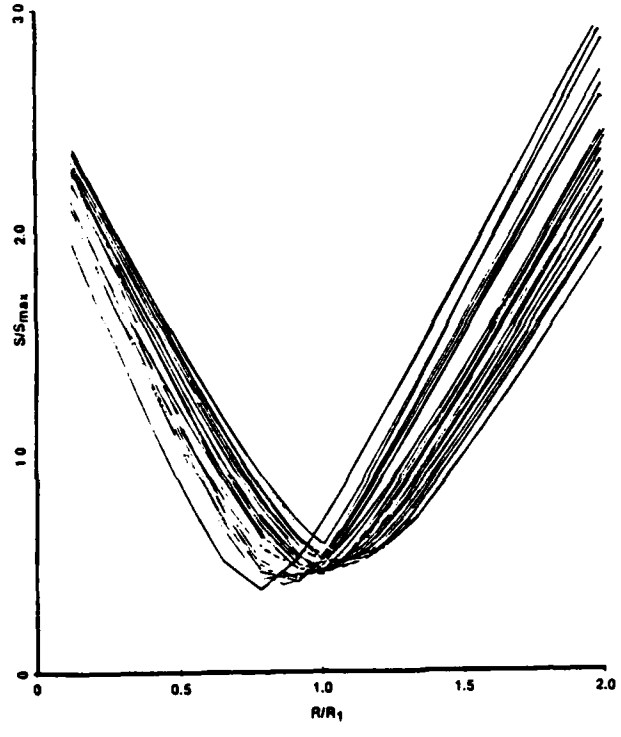

Figure 8. Normalized Speed vs Normalized Range Constraint ($\theta=\theta_5$) for 30 Noise Sequences

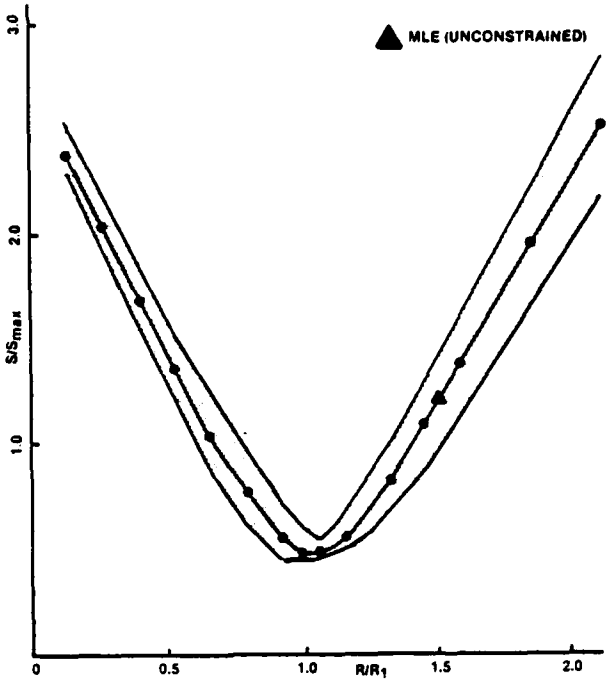

Figure 9. Region of Minimal σ_β^2

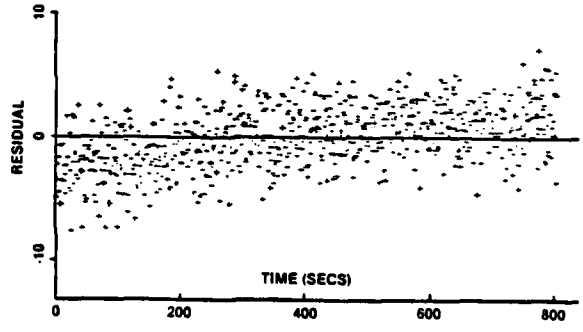

Figure 10. Bearing Residual vs Time; $\theta=\theta_5$, $R/R_{true}=2.4$, $S/S_{true}=1.0$

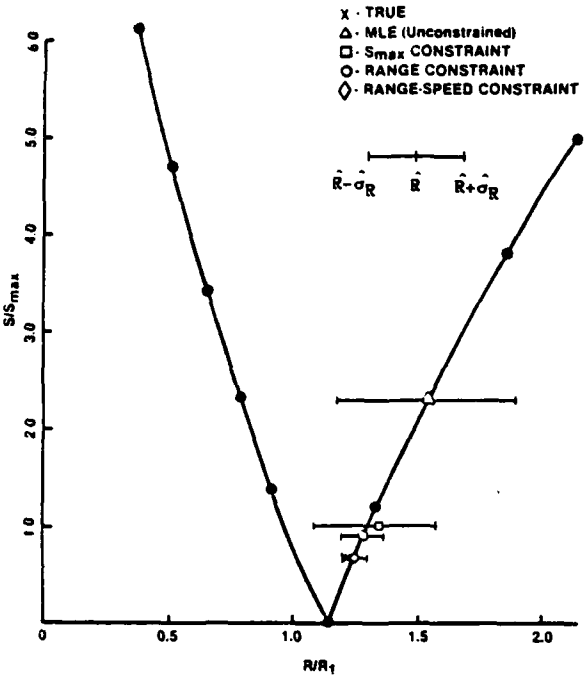

Figure 11. Solution Enhancement via Utilization of Heuristic Information ($\theta=\theta_1$)

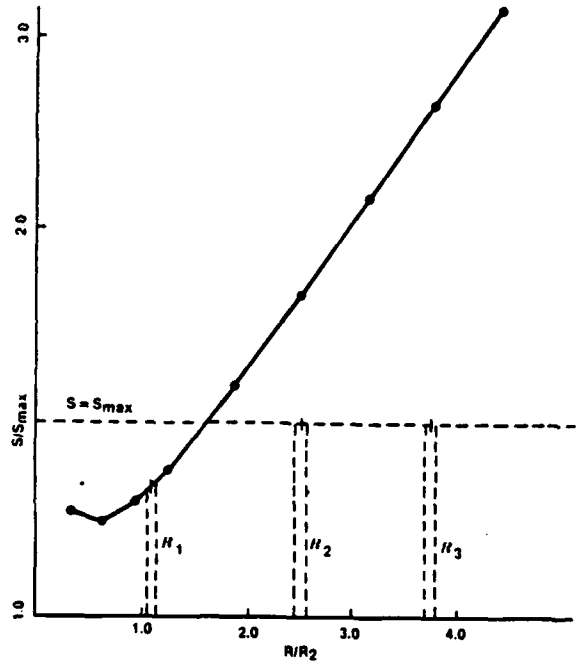

Figure 12. Solution Selection via Constrained Estimation ($\theta=\theta_6$)

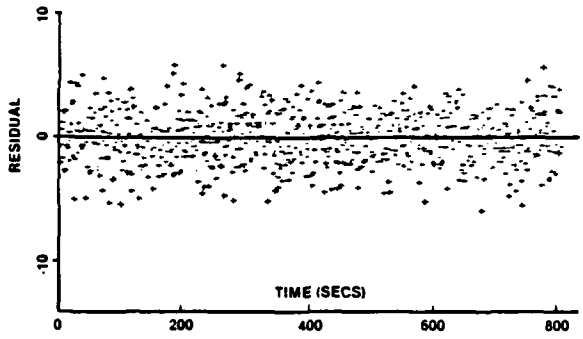

Figure 13a. Bearing Residual vs Time; $\theta=\theta_6$, $R/R_{true}=1.0$, $S=S_{true}<S_{max}$

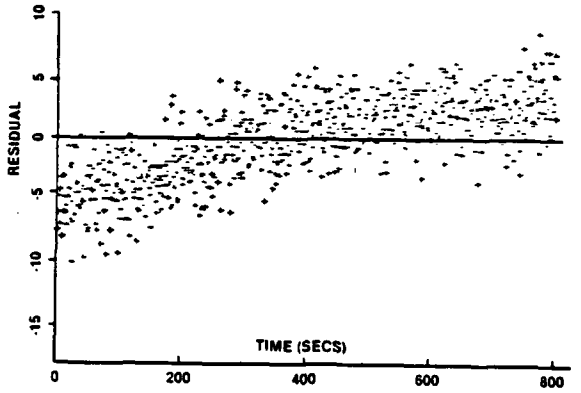

Figure 13b. Bearing Residual vs Time; $\theta=\theta_6$, $R/R_{true}=2.3$, $S=S_{max}$

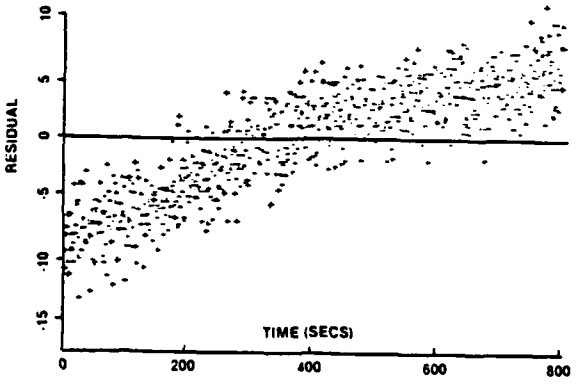

Figure 13c. Bearing Residual vs Time; $\theta=\theta_6$, $R/R_{true}=3.4$, $S=S_{max}$

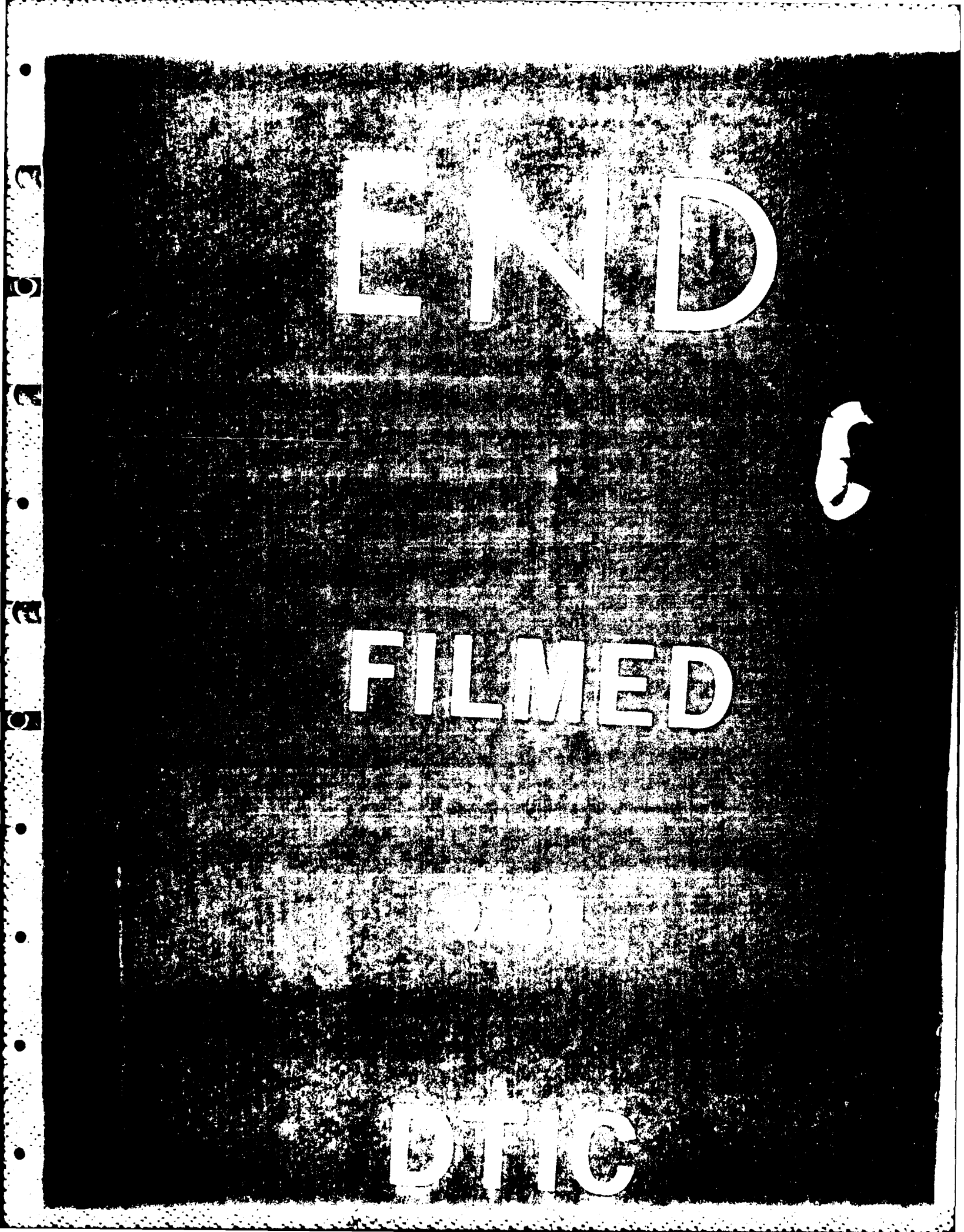
END
FILMED
DTIC